Original Article

Visualizing Stable Features in Live Cell Nucleus for Evaluation of the Cell Global Motion Compensation

(cell global motion compensation / UV laser bleaching / image registration / stable features / algorithm evaluation)

D. V. SOROKIN[1], J. SUCHÁNKOVÁ[2], E. BÁRTOVÁ[2], P. MATULA[1]

[1]Centre for Biomedical Image Analysis, Faculty of Informatics, Masaryk University, Brno, Czech Republic
[2]Institute of Biophysics, Academy of Sciences of the Czech Republic, v. v. i., Brno, Czech Republic

Abstract. The compensation of cell motion is an important step in single-particle tracking analysis of live cells. This step is required in most of the cases, since the movement of subcellular foci is superimposed by the movement and deformation of the cell, while only the local motion of the foci is important to be analysed. The cell motion and deformation compensation is usually performed by means of image registration. There are a number of approaches with different models and properties presented in the literature that perform cell image registration. However, the evaluation of the registration approach quality on real data is a tricky problem due to the fact that some stable features in the images with a priori no local motion are needed. In this paper we propose a methodology for creating live cell nuclei image sequences with stable features imposed. The features are defined using the regions of fluorescence bleaching invoked by the UV laser. Data with different deformations are acquired and can be used for evaluation of the cell image registration methods. Along with that, we describe an image analysis technique and a metric that can characterize the quality of the method quantitatively. The proposed methodology allows building a ground truth dataset for testing and thoroughly evaluating cell image registration methods.

Received June 27, 2014. Accepted July 27, 2014.

This work was partially supported by the Czech Science Foundation [P302/12/G157 to EB and JS], the European Social Fund and the Ministry of Education, Youth and Sports of the Czech Republic [CZ.1.07/2.3.00/30.0030 to DVS and PaM].

Corresponding author: Dmitry V. Sorokin, Centre for Biomedical Image Analysis, Faculty of Informatics, Masaryk University, Botanická 68a, 602 00, Brno, Czech Republic. Phone: (+420) 549 497 684; e-mail: sorokin@fi.muni.cz

Abbreviations: DMEM – Dulbecco's modified Eagle's medium, ROI – region of interest, WLL – white light laser.

Introduction

Cell nucleus represents a fundamental nuclear organelle whose functions dictate all cellular processes, including cell proliferation, differentiation and cell death – apoptosis. Thus, studies of nuclear processes, such as replication, transcription, splicing, and DNA repair are important from the view of understanding the balance between physiological/pathophysiological nuclear events. Information on the localized movement of nuclear particles, foci and bodies can contribute to the knowledge of the functional properties of nuclear architecture (Muratani et al., 2002; Stixová et al., 2011; Foltánková et al., 2013).

The critical step for the analysis of movements within the nucleus is the motion compensation of the cell as a whole. The first approaches to the cell motion compensation considered the cell/nucleus as a rigid body and estimated the translation and rotation of the cell between the frames (Gerlich et al. 2001; Matula et al., 2006; Wilson et al. 2006). However, the cell cannot be considered as a rigid body and that is why non-rigid approaches have been invented (Mattes et al. 2006; De Vylder 2011; Kim et al. 2011; Sorokin et al. 2014). In the non-rigid approaches, the dense vector deformation field estimating the motion and deformation of the cell is constructed. To perform the compensation of the cell motion, the obtained deformation field is inverted and applied to the initial sequence, thus normalizing each frame of the sequence to the initial time moment. This process is also referred to as image registration.

Even though the cell motion compensation approaches are based on reasonable and realistic assumptions, one may ask how good or bad the approach is. Their evaluation is not an easy task, because the real cell motion is unknown. The common way to evaluate an approach is to track some stable points in the nucleus, compensate the cell motion with the given approach (the location of the stable points changes due to the cell motion compensation) and measure the residual motion of the tracked stable points (Kim et al. 2011; Sorokin et al. 2014). In the ideal case the residual motion should be absent.

Thus, the less local mobility of the stable points remains, the better the approach is. The stable points are usually represented by some protein foci that are in general not guaranteed to be without local mobility. The tracking of the stable points is usually provided by an expert in the field (e.g., placed by mouse clicking). This solution has two main flaws: (1) the placement of the points is expert-dependent and precisely unreproducible, (2) there is no guarantee the points really correspond to stable key-points. For example, if the expert puts a mark at a locally moving structure.

In this paper, we describe preparation of live nucleus video sequences with well-defined stable features that can be used for evaluation of the cell motion compensation algorithms. The main idea is to bleach a regular grid using a UV laser in chromatin visualized by H2B-GFP. The axes of the bleached stripes are algorithmically detected in every frame. Chromatin is considered by its definition to be the basic structure in the cell nucleus, while the stripes cover the whole nucleus, and thus they are considered to be stable features in the whole sequence. Also, we bleach the stripes in a protein channel with a subtle recovery after photobleaching, so the sharpness and stability of the stripes in time is prominent. Additionally, we propose an image processing technique that allows detecting three types of stable features in the acquired data. Exploiting the evaluation metrics used in Kim et al. (2011); Sorokin et al. (2014) and an introduced metric for the line features we showed the suitability of the features for thorough evaluation of the nucleus motion compensation methods.

Material and Methods

Cell lines and cell treatment

HeLa cells, stably expressing histone H2B tagged by GFP, were a generous gift from Dr. Marion Cremer, Ludwig Maximilian University in Munich, Germany. This adherent cell line was cultivated in Dulbecco's modified Eagle's medium (DMEM, Sigma-Aldrich, Prague, Czech Republic), supplemented with antibiotics and 10% foetal calf serum at 37 °C in a humidified atmosphere containing 5% CO_2. For induction of pronounced cell movement and nuclear deformation, we used deprivation of CO_2.

Cell transfection by plasmid DNA

We used plasmids encoding GFP-HP1β (#17651; Addgene, Cambridge, MA) and GFP-tagged lamin A (#17662; Addgene), but the sequences of both genes were re-cloned into the mCherry-pBABE puro vector. For transient cell transfection we used the METAFECTENETMPRO transfection kit (Biontex Laboratories GmbH, Planegg, Germany). We transfected the cells with 2–5 μg plasmid DNA. Amplification of plasmid DNA was performed by the use of chemically competent *E. coli* DH5α bacteria, and plasmid DNA was isolated with the Qiagen Plasmid Maxi Kit (#121693, Qiagen, Bio-Consult, Czech Republic).

Photobleaching used for bioinformatic analyses

Living cells, cultivated on microscope dishes (μ-Dish 35mm Grid-500 (#81166, Ibidi, Planegg, Germany), were placed into a cultivation hood (EMBL, Heidelberg, Germany) tempered to 37 °C. The air-stream cultivation hood was used to provide 5% CO_2, so that we were able to maintain optimal cell growth, but we increased the cell movement by deprivation of CO_2.

After cell stabilization in the cultivation hood, we bleached the regions of interest (ROIs) of the defined grid-shape. We bleached histone H2B tagged by GFP. A-type lamins or HP1β, both tagged by mCherry, were used as additional proteins of interest. Primarily, GFP-H2B was selected for the experimental approach leading to subsequent bioinformatic processing. It is well-known that GFP-H2B is characterized by a subtle recovery after photobleaching (Gilchrist et al., 2004; Meshorer et al., 2006), and thus was suitable for the intended image analysis. For the bleaching experiments we used argon laser (488 nm of the wavelength); 100% laser intensity at AOTF. For forthcoming scanning, white light laser (WLL; Leica, Mannheim, Germany, 470-670 nm in 1-nm increments) was set to 15 % of maximal intensity. For bleaching and time-lapse microscopy we used a Leica SP5-X confocal microscope (Leica), equipped with objective HCX PL APO lambda blue 63.0 x; numerical aperture (N.A.) = 1.4; OIL UV. Cell nuclei were acquired at the following settings: 512 × 512 pixels, 400 Hz, conventional mode in one direction, 4 lines, zoom 8. Cell nuclei with grids, bleached in GFP-H2B, were monitored each 6 s for 10-15 min.

Image sequences

After the acquisition we selected eight image sequences: three sequences showing histone H2B tagged by GFP with HP1β tagged by mCherry (further referred to as SA1, SA2 and SA3), three sequences showing histone H2B tagged by GFP with A-C-type lamins tagged by mCherry (further referred to as SB1, SB2, SB3), and two sequences showing histone H2B tagged by GFP with A-type lamin tagged by mCherry (further referred to as SC1, SC2). Due to the decreasing image quality with time, the sequences were cut in time depending on the noise level and fluorescence decrease. As a result, the SA sequences contain 41, 30 and 140 frames, the SB sequences contain 25, 22 and 42 frames, and the SC sequences contain 42 and 26 frames, respectively. The lateral size of each frame is 512 by 512 pixels.

Image analysis

We segmented the nucleus using an algorithm combining intensity and edge information of the green channel. The mCherry channel was used for visual validation of the segmentations. Image thresholding led to a binary mask with holes and stripes because of the weak intensity in the bleached regions. Morphological closing and

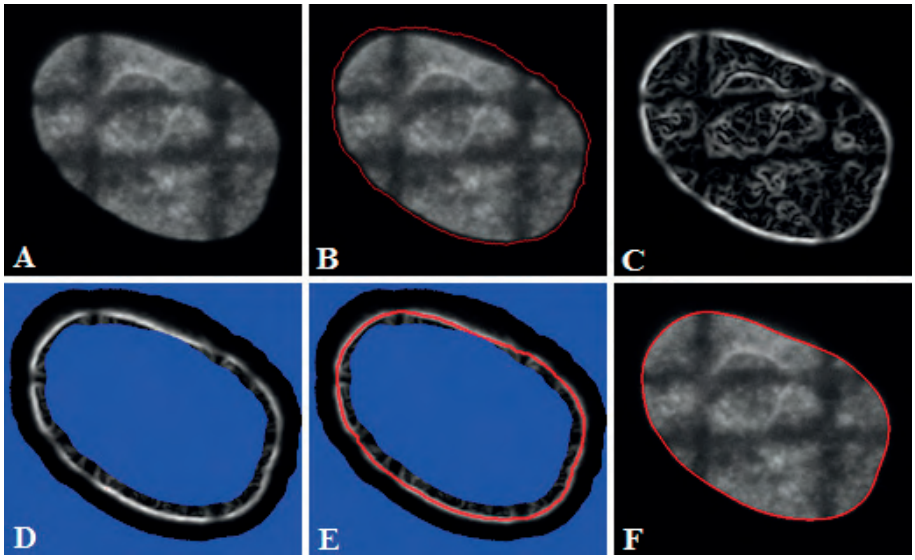

Fig. 1. Nucleus segmentation. **A.** Input image. **B.** Contour obtained by the thresholding-based algorithm. **C.** Gradient magnitude image. **D.** Two minima (blue regions) imposed in the gradient magnitude image. **E.** Watershed line between two minima. **F.** Input image overlaid with the smoothed watershed line.

hole-filling of the mask was necessary, as it improved the mask, but the mask boundary did not exactly follow the nucleus boundary in general. That is why we used the morphological watershed algorithm applied to the gradient magnitude image, where we imposed two minima forming a band around the mask boundary. The idea was to use the edge information, which was weak but still apparent in the bleached regions, to compute the precise nucleus boundary (Fig. 1).

Every sequence was processed to detect the stable features that can be used for evaluation of the registration algorithm. We used three types of features (Fig. 2). The features were detected in the green channel of the sequences. First, we detected the curves representing the grid-like structure bleached in the nucleus (further referred to as line features). The line features were detected in every frame separately using the minimal paths' approach (Cohen et al., 1997) with the potential defined as the Gaussian smoothed ($\sigma = 3$) green channel intensity of the frame and starting and ending points located in the bleached region on the nucleus boundary.

To detect the starting and ending points of the curves we used the following approach. First, we constructed the 1D green channel intensity profile of the image along the closed contour-located R pixels (R varied between 3 and 7, depending on the sequence) towards the interior of the nucleus from its boundary (Fig. 2). Then the profile was smoothed with the Gaussian, all local minima were detected and the eight lowest minima were selected as candidates. The image points (x,y) corresponding to the candidate minima were checked whether they matched the bleaching pattern (two parallel lines orthogonally crossed with two other parallel lines) and grouped into four pairs defining the starting and ending point for each curve. If at least one of the points did not match the pattern, another local minimum of the smoothed 1D intensity profile was selected as a candidate. The candidate was selected in a way that its corresponding image point (x,y) was the closest point to the corresponding starting or ending point in the previous frame. The line features were represented as a 2D piecewise linear curve with subpixel precision. After the line features were detected in every frame, the intersections of the line features were computed. The obtained intersection points were considered as stable features further referred to as inner-point features. The starting and ending points of each line feature were also considered as

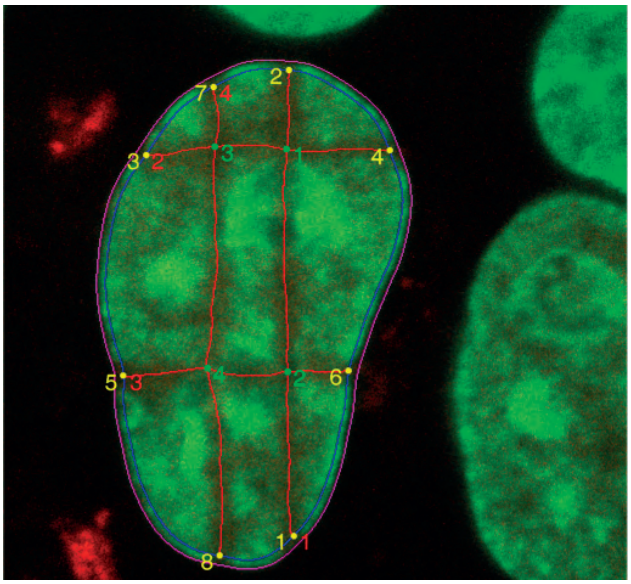

Fig. 2. The features depicted in the first frame of sequence SA2. The magenta line represents the nucleus boundary, the blue line represents the closed contour along which the intensity profile for boundary-points' detection is taken, the red lines represent the line features, the green dots represent the inner-point features, and the yellow dots represent the boundary-point features.

stable features, further referred to as boundary-point features.

Evaluation metrics

To evaluate the quality of the given image registration approach we applied the deformation fields to the features normalizing their position to the position in the first frame. The quality of the registration corresponds to the distance between the transformed position of the feature in the i-th frame and the position of the feature in the first frame: the lower the distance, the higher the quality of the registration approach. We defined the following error measures for the inner-point and boundary-point features (Sorokin et al., 2014). The registration error $e_i^k = \|\mathbf{p}_i^k - \mathbf{p}_i^1\|$ defines the Euclidean distance between the i-th feature point in the k-frame $\mathbf{p}_i^k$ and i-th feature point in the first frame $\mathbf{p}_i^1$. The registration error averaged over features $\overline{e^k} = \frac{1}{K}\sum_{i=1}^{K}\|\mathbf{p}_i^k - \mathbf{p}_i^1\|$, where K is the number of features, and the registration error averaged over features and time $\overline{e}_{mean} = \frac{1}{N}\frac{1}{K}\sum_{k=0}^{N-1}\sum_{i=1}^{K}\|\mathbf{p}_i^k - \mathbf{p}_i^1\|$, where K is the number of features and N is the number of frames. The registration errors for line features are defined in a similar way except that the distance between the curves is computed as the area of the polygon formed by the two lines. The polygon area approximates the standard L1 distance between the curves.

Results

In this work we obtained eight 2D image sequences representing deforming nuclei with stable landmark regions that correspond only to the motion and deformation of the nuclei. Using the proposed technique we detected three types of features: line features, inner-point features and boundary-point features. To illustrate how the obtained features can be used for evaluation of the nucleus global motion compensation algorithms we applied the registration approach presented in Sorokin et. al. (2014) to our data and compared it with the results for non-registered sequences. The main idea of the approach was to use the deformation of the nucleus contours to model the deformation of the entire nucleus by solving the Navier equation with Dirichlet boundary conditions. The obtained solution represents the global motion of the nucleus, which is afterwards eliminated from the motion of the features. The dependence of $\overline{e^k}$ on time for different features of the sequence SA1 is shown in Fig. 3. The values of $\overline{e}_{mean}$ for different features and datasets are shown in Table 1.

Discussion

The presented results show an approximately 2-fold decrease in the mobility of the detected features after the application of the registration approach. The absolute values of the errors are consistent with the results obtained in the previous works (Kim et al., 2011; Sorokin et al., 2014), where some point features were manually selected by the experts. However, the proposed methodology for constructing the evaluation datasets for cell global motion compensation seems more advantageous in reliability and time required for the processing of the data since the feature selection process is automated. The features detected by the proposed approach represent both the periphery of the nucleus and its interior, which can be used for testing different aspects of the cell image registration algorithms. In addition, a new kind of

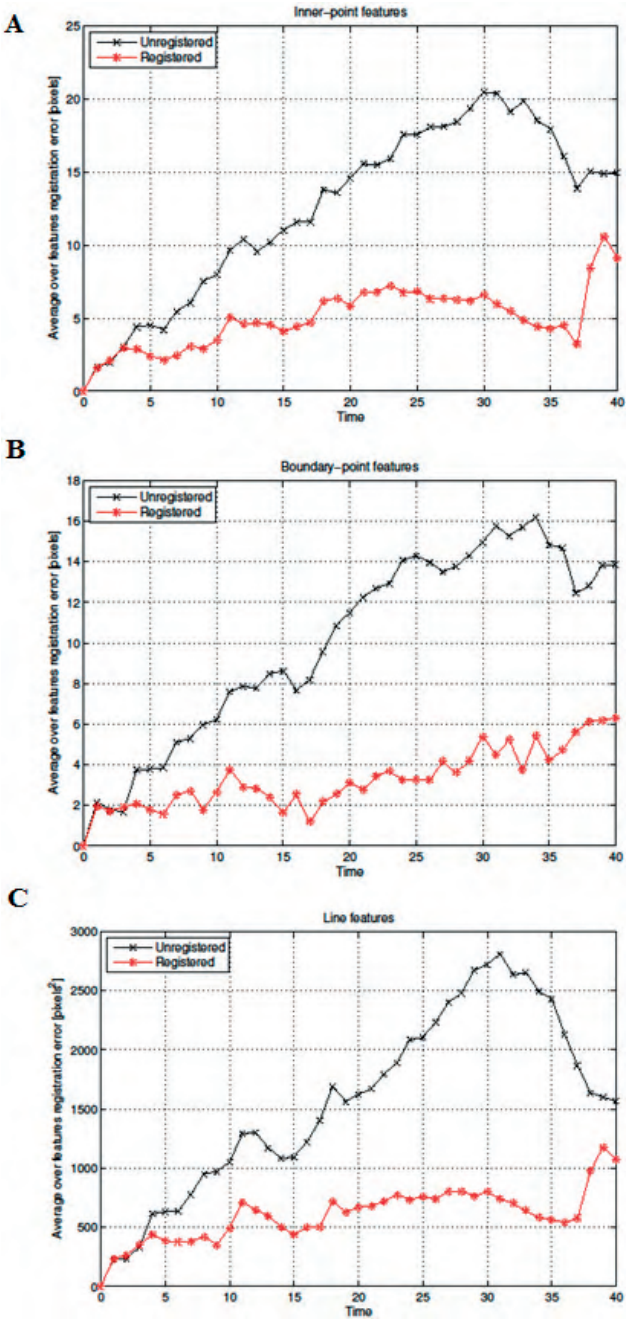

Fig. 3. The $\overline{e^k}$ error graphs for the sequence SA2. **A.** For inner-point features. **B.** For boundary-point features. **C.** For line features.

Table 1. The values of $\bar{e}_{mean}$ for different features and datasets

	SA1	SA2	SA3	SB1	SB2	SB3	SC1	SC2
$\bar{e}_{mean}$ for inner-point features, [px]								
Unregistered	12.43	5.30	7.70	6.67	2.88	7.55	15.97	4.88
Registered	4.96	3.70	4.74	2.81	2.16	3.73	10.15	2.27
$\bar{e}_{mean}$ for boundary-point features, [px]								
Unregistered	10.00	6.79	9.43	7.95	3.28	9.84	18.02	5.23
Registered	3.29	4.75	4.51	3.37	2.81	3.44	8.28	2.60
$\bar{e}_{mean}$ for line features, [px2]								
Unregistered	1554.16	1211.30	1031.18	691.50	436.63	868.59	2037.56	506.31
Registered	603.65	703.91	674.92	313.77	373.64	412.15	1194.81	224.83

features (line features) was presented. This type of features was not used in the previous works. However, this type of features looks promising for the evaluation purposes because of its large-scale character covering the whole nucleus. To conclude, our preliminary results look promising and show the ability to use the proposed methodology for evaluation of the cell global motion compensation algorithms, while thorough analysis of the stability of the obtained features and comparison of different cell image registration approaches to the proposed datasets is a matter of future work.

References

Cohen, L. D., & Kimmel, R. (1997) Global minimum for active contour models: a minimal path approach. *Int. J. Comput. Vis.* **24,** 57-78.

De Vylder, J., De Vos, W. H., Manders, E. M., Philips, W. (2011) 2D mapping of strongly deformable cell nuclei based on contour matching. *Cytometry A*, **79**, 580-588.

Foltánková, V., Matula, P., Sorokin, D., Kozubek, S., & Bártová, E. (2013) Hybrid detectors improved time-lapse confocal microscopy of PML and 53BP1 nuclear body colocalization in DNA lesions. *Microsc. Microanal.* **19**, 360-369.

Gerlich, D., Beaudouin, J., Gebhard, M., Ellenberg, J., Eils, R. (2001) Four-dimensional imaging and quantitative reconstruction to analyse complex spatiotemporal processes in live cells. *Nat. Cell Biol.* **3**, 852-855.

Gilchrist, S., Gilbert, N., Perry, P., Östlund, C., Worman, H. J., Bickmore, W. A. (2004) Altered protein dynamics of disease-associated lamin A mutants. *BMC Cell Biol.* **5**, 46.

Kim, I. H., Chen, Y., Spector, D. L., Eils, R., Rohr, K. (2011) Nonrigid registration of 2-D and 3-D dynamic cell nuclei images for improved classification of subcellular particle motion. *IEEE Trans. Image Process.* **20**, 1011-1022.

Mattes, J., Nawroth, J., Boukamp, P., Eils, R., & Greulich-Bode, K. M. (2006) Analyzing motion and deformation of the cell nucleus for studying co-localizations of nuclear structures. *Proc. IEEE Int. Symp. Biomed. Imaging: Nano to Macro (ISBI'2006)*, 1044-1047.

Matula, Pe., Matula, Pa., Kozubek, M., & Dvorak, V. (2006) Fast point-based 3-D alignment of live cells. *IEEE Trans. Image Process.* **15**, 2388-2396.

Meshorer, E., Yellajoshula, D., George, E., Scambler, P. J., Brown, D. T., Misteli, T. (2006) Hyperdynamic plasticity of chromatin proteins in pluripotent embryonic stem cells. *Dev. Cell* **10**, 105-116.

Muratani, M., Gerlich, D., Janicki, S. M., Gebhard, M., Eils, R., & Spector, D. L. (2001) Metabolic-energy-dependent movement of PML bodies within the mammalian cell nucleus. *Nat. Cell Biol.* **4**, 106-110.

Sorokin, D. V., Tektonidis, M., Rohr, K., & Matula, P. (2014) Non-rigid contour-based temporal registration of 2D cell nuclei images using the Navier equation. *Proc. IEEE Int. Symp. Biomed. Imaging: Nano to Macro (ISBI'2014)*, 746-749.

Stixová, L., Bártová, E., Matula, P., Daněk, O., Legartová, S., Kozubek, S. (2011) Heterogeneity in the kinetics of nuclear proteins and trajectories of substructures associated with heterochromatin. *Epigenetics Chromatin*, **4**, 5.

Wilson, C. A., Theriot, J. A. (2006). A correlation-based approach to calculate rotation and translation of moving cells. *IEEE Trans. Image Process.* **15**, 1939-1951.